JNBT
©2005INBDK

JNBT, Vol 2, No 2, pp. 59-65

Computational Studies of Carbon Nanostructures

Noejung Park*

Department of Applied Physics & Institute of Nanosensor and Biotechnology, Dankook University, Seoul, Korea

ABSTRACT

The paper reviews author's recent theoretical works on the carbon nanostructures including fullerenes and nanotubes. The developments of the ***ab initio*** method using the localized basis set are also described with an introduction to the requirement for large-sized first-principles calculations. The total energy calculations on the sp^2-bonded carbon structures show that the energetics regarding the incorporation of pentagonal rings favors the curvature of the C_{240} and, consequently, the cap of the (10,10) nanotube. As a study aiming at a practical application, field emission properties of the carbon nanotube are investigated. A general introduction to the various advantages of the carbon nanotube as an electron field emitter is followed by detailed studies on the oxygen adsorption effects.

Key words : nanostructure, carbon nanotube, first-principles calculations

Ⅰ. Introduction

Ever since the first discovery of fullerenes (1) and carbon nanotubes (2), the sp^2-bonded carbon nanostructures have been under intensive scrutiny and numerous mutations of them have been synthesized (3-6). Although the local atomic structure is the same with that of graphite, various unprecedented phenomena, depending sensitively on the overall topology, have attracted wide range of researchers so far. While the interests of fullerene molecule itself lay in its remarkable stability and beautiful symmetry, various electronic behaviors of the carbon nanotube and the crystallized form of fullerenes, ranging from semiconductor to metals (7-9), and to superconductors (10,11), have triggered suggestions for numerous potential applications. Robust one-dimensional shape of the carbon nanotube, in addition to its exceptional chemical and mechanical stability, have also attracted much interests for particular applications, including field emission tips (12,13), molecular electronic devices (14), and probing tips (15). Among them the field emission display using the carbon nanotube emitters is approaching a commercialized product.

Since most physical properties of this nanoscale material, whose size is of several tens or several hundreds of atoms, can properly be described by quantum mechanics, and some of them manifest quite distinguishable properties from classical ones (16), the computational approach have been believed to contribute greatly to this field of study. The agreements between theories and experiments with a high precision have stimulated a further scientific investigation in the carbon nanotubes (17,18). However, a naive application of the first-principles calculation methods often confronts with a severe limitation because of its high computational costs. Although the ***ab initio*** method based on the density functional theory (19,20) has been successfully developed aiming at the solid states, nanoscale materials, whose structure is not a periodic one, and can be regarded as a large molecule rather than a solid, usually require much large-sized computations. These days several authors have tried to develop large-sized calculation methods in order to have a more realistic simulation for these nanoscale materials (21).

In this review article we present recent theoretical works on the carbon nanotubes and fullerenes as well as the devel-

* Corresponding author :
Noejung Park
Tel : +82-2-799-1383
Fax : +82-2-799-6082
E-mail : noejung@dku.edu

opment of large-scale first-principle calculation methods. In the next section, a brief description for the first-principles electronic structure calculatons will be presented and followed by a demonstration showing that a localized basis set can be successfully employed to deal with a large-sized system with a reasonable accuracy. In section III, we present a study on the energetics of the curved sp^2-carbon nanostructures. We show that the energetics regarding the incorporation of pentagonal rings does a crucial role in the relative stability among the isomers and mostly favor the capped (10, 10) tube over a smaller or larger nanotube. In the last section, we review the field emission properties of the carbon nanotube and present a detailed study on the oxygen adsorption effects. We show that the adsorption can increase the local electric field as well as the local density of states, which can positively affect the electron field emission from carbon nanotubes.

Ⅱ. Ab initio methods for nanoscale materials

Density functional theory (19) states that the total energy of N-electrons system, which i s in its ground state, is unique functional of charge density ρ, as $E_T[\rho] = T[\rho] + \int u\rho\, d^3\vec{r}$, where $T[\rho]$ is kinetic energy of electrons and v is the external potential. The interaction energies between the electrons can be expressed as. $U[\rho] = \frac{1}{2}\iint \frac{e^2\rho(\vec{R}_1)\rho(\vec{R}_2)}{|\vec{R}_1 - \vec{R}_2|}\, d^3\vec{R}_1 d^3\vec{R}_2 + E_{xc}[\rho]$ Assuming that the ground state charge density can be ex panded by N orbitals, $\rho = \sum_{i=1}^{N} |\psi_i|^2$, the eigenvalue equation for ψ_i can be constructed and eventually the total energy can be calculated; The Euler-Langrange equation which minimize the total energy with respect to the variation of $\{\psi_1.\psi_2.\cdots\cdots\psi_N\}$ produce N single particle equations (20), as $(-\overrightarrow{\nabla}^2 + u(\vec{r}) + v_h(\vec{r}) + \mu_{xc}[\rho])\psi_i = \epsilon_i\psi_i$, where $u_h\vec{r})$ and $\mu_{xc}[\rho]$ are potentials describing the electron-electron interaction energy $U[\rho]$. The most standard method to attack this equation is to expand the Kohn-Sham orbital ψ_i with a set of plane waves (22). Electronic states in solids can neatly be described by the plane waves, whose wave numbers are integer multiples of the reciprocal lattice vectors of the crystal.

However, nanostructures are not three-dimensional crystal, and the plane wave calculations on them often confront with huge computational costs. For example, in the calculation of dimerized fullerenes which is shown in **Fig 1 (a)**, we need a 2×10^6 plane waves for a reasonably converged energy value, which takes about 20~30 CPU hours for a self-consistency step in CrayT3E supercomputer. A significant curtailment of CPU time can be obtained by expanding the Kohm-Sham orbital ψ_i with a localized basis. In **Fig 1 (b)**, we present the cohesive energies of small fullerenes calculated with the plane-wave basis and the atomic orbital-like localized basis set (23). We find that the accuracy of the calculations with the localized basis is in 0.01 eV/atom, whose CPU time is reduced to one fortieth of that of the plane waves.

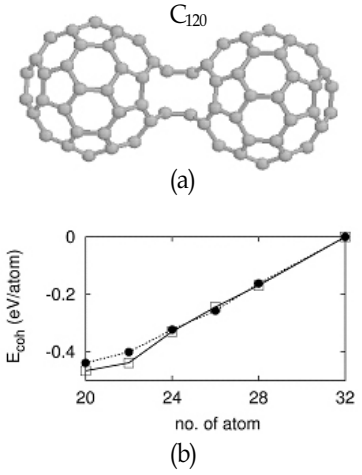

Fig 1. (a) C_{120} in the intermediate stage of two fullerenes fusion (56). (b) Cohesive energies of small fullerenes. Filled circles are the results of the plane-wave method and the squares are those of the localized-basis method.

Ⅲ. Energetics of curved graphitic structures

Among various forms of carbon nanotubes or clusters in nano scales, the single-walled carbon nanotube (SWNT) has attracted much attention because of its unique structural and electronic properties. However, the study of single-walled nanotubes has often been hindered by the lack of knowledge in the basic growth mechanism of carbon nanotubes and related clusters. Recent experiments (24-29) have reported that the diameters of the single-walled carbon nanotubes have a

narrow distribution range around that of the (10, 10) tube.

Several models of the nanotube growth (30-32) have suggested that the formation of the single-walled nanotubes and fullerenes are initiated by the graphitic bowls, and the energetics of large carbon clusters should play a crucial role. While a single-walled nanotube is frequently described as a rolled-up graphitic sheet, it may as well be considered as an elongated fullerene when it is capped. Since the fullerene itself is another important form of carbon clusters, the energetics of large fullerene in general including the capped carbon nanotubes should be useful in understanding the initial growth process of nanotubes and its diameter distributions.

In earlier work, Adams and co-workers (33) showed that a key factor in determining the energetics of large fullerenes and carbon nanotubes was the nonplanarity of the graphitic sheet incurring incompleteness of the π-bonding. Based on the empirical formula derived from the computational results, they concluded that the spherical fullerenes were energetically favored over the tube-like elongated fullerenes, i.e., capped nanotubes. Since, however, theoretical studies of large carbon clusters demand enormous electronic structure calculations, the fully self-consistent first-principles calculations have been restricted to relatively small system size. So far many calculations on the large carbon clusters were done by classical continuum theory (34), or molecular dynamics with the three-body potential (35), or so-called *O(N)* methods with the non-self-consistent Harris functional formalism (33,36,37).

However, a fully self-consistent first-principles calculations in this work show somewhat different results from the predictions of the previous works. The total energies of the fullerenes with respect to that of the infinite graphene sheet are presented in **Fig 2 (a)**. Compared to the previous results (33), the energy curve of the spherical fullerenes stays flat in the range of $N > 240$. In order to explain this phenomenon, here we note two different strain sources: one from the curvature effect and the other from the bond length change of the pentagons. The pure curvature effect can be traced to the angle changes between the nearly paral lel $\pi-$orbitals. In case of the infinite (n, n) tubes, it can be expressed by the form of $\varepsilon_{tube} \approx \varepsilon' \left(\frac{d}{r}\right) = \frac{\varepsilon_1}{n^2}$, where d is the C-C bond length and r is the tube radius. Indeed the results of the first-principles calculations are extremely well fitted to this simple formula with a parameter $\epsilon_1 = 4.12$ eV (21). Similarly, the curvature energy of the spherical fullerene can be mod eled as $\varepsilon_{tube} \approx \varepsilon'' \left(\frac{d}{r}\right)^2 = \frac{\varepsilon_1}{N}$, where the r is the radius of the fullerene. Note that the surface area of the fullerene $(4\pi\gamma^2)$ is proportional to the total number of atoms N. In **Fig 2 (a)**, it is obvious that the calculated N-dependence of the total energy deviates significantly from the above simple formula, implying that the curvature effect alone is not sufficient for the description of the energetics of fullerenes.

Another important contribution to the total energy of the fullerenes distinct from the curvature effect comes from the strain in the pentagon region. The origin of such strain can be sought in the geometry of an isolated graphitic cone. A cone here is defined to be a structure where a pentagon is surrounded by hexagonal network. If the cone angle θ, which is shown in **Fig 2 (b)**, is forced to deviate from its equilibrium value (θ_0), an extra energy cost which we call "pentagonal strain energy" is required. While the curvature energy arises from the changes in the bond angle, the cone energy comes from the change of the C-C bond lengths from the values of the equilibrium. Through extensive ***ab initio*** calculations, we find that the pentagonal strain energy can be modeled by assuming that the bond length change is effectively confined to 5 bonds forming the pentagon. As shown in the schematic illustration of **Fig 2 (c)**, the bond length change of the pentagon (δ) is related to the length of the cone edge (L) and the angle change $(\theta - \theta_0)$, which is assumed to be small, as follows;

$$\delta = 2L(\cos\theta - \cos\theta_0) \propto \sqrt{N_{cone}(\theta - \theta_0)}$$

The length L of the cone edge is approximately proportional to the square root of the number of atoms belonging to the cone (N_{cone}). The pentagonal strain energy in the spherical fullerene, in which 12 cones are interconnected by the intermediate graphitic region, can be expressed as

$$E_{cone} = 12 \times \frac{k'}{2} N_{cone}(\theta - \theta_0)^2 \approx 12 \times \frac{k}{2} N_{cone}\left(\frac{1}{\sqrt{N}} - \frac{1}{\sqrt{N}}\right)^2,$$

where we assumed that the fullerenes are nearly spherical and, hence, $\theta \propto 1/r$ and $r \propto \sqrt{N}$. Eventually, the energy model form for fullerene including curvature effect as well as

pentagon effect becomes as

$$\epsilon_{fl} = ((N-60)\epsilon_{cf} + E_{cone})/N.$$

Here we note that the pentagon itself remains as a regular polygon independently of the size of the fullerene, and hence, we ignore the angle change between the π-orbitals within the pentagons and the corresponding curvature energy. Only the *(N-60)* atoms which do not participate in the pentagons contribute to the curvature energy. The solid line in **Fig 2 (a)** using this energy formula really fits well the calculated points. To check the validity of our fit, we have calculated an extra point at *N=540* not included in the fitting procedure.

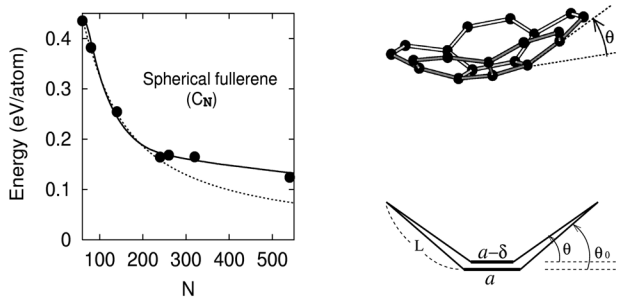

Fig 2. (a) Total energy of the spherical fullerene with respect to infinite graphene sheet. Filled circles are the results of the self-consistent calculations, and the solid line is fitted curve of the model described in the text (b). A graphitic cone structure. (c) A schematic illustration of the bond length change of the pentagon (thick horizontal bars) accompanied by the cone angle change.

Now we are going to construct the energy model for the single-walled carbon nanotube with caps. Here, we assume the cap of the nanotube is a hemisphere of spherical fullerene; for example, the cap of (5,5) tube is the hemisphere of C_{60}. By summing up the energy contribution from the pure tube region of $(N\text{-}N_{cap})$ atoms and the fullerene-like cap regions of N_{cap} atoms, the total energy per atom is

$$\varepsilon_{cap\text{-}tube} = \left(\frac{N-N_{cap}}{N}\right)\varepsilon_{tube} + \left(\frac{N_{cap}}{N}\right)\varepsilon_{fl}.$$

The energy curves of nanotubes and fullerenes using this formula are presented in **Fig 3**. Three data points (one at (5,5) tube and two at (10,10) tube) are independently calculated to verify the energy formula.

Contrary to the prediction of the previous works, the energy curve of the (10,10) nanotube stays below that of the fullerene. This fact indicates that (10,10) nanotube is not only more stable than fullerenes, but it is more stable than smaller or even larger nanotubes as well. Since our energy model only cares about the size of the cap, the chirality does not matter. Thus, for example, the (18,0) nanotube capped with hemisphere of C_{240} can be as stable as the (10,10) nanotube. Our energy model suggests that the decisive factor of the diameter of the single-walled nanotube is the energetics of the cap at the initial stage of formation. For example, if we consider a graphitic bowl of a few hundred carbon atoms ($N \approx 300$), the total energy of the (10,10) tube-like elongated fullerene is lower than its isomeric spherical fullerene by about 1 Ry.

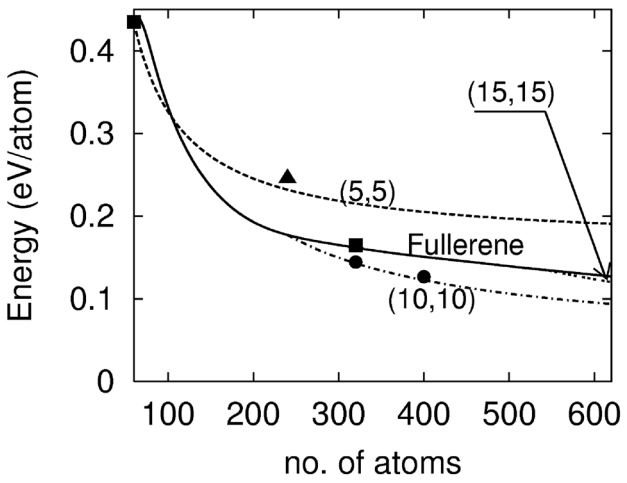

Fig 3. The *N*-dependence of the energy for the capped (*n,n*) nanotubes (dashed line for (5,5), dash-dotted line for (10,10), and dotted line for (15,15) tube, respectively.) in comparison with spherical fullerenes (solid line). The triangle, squares, and circles are the results of the self-consistent calculations.

Ⅳ. Field emission properties of the carbon nanotube

From the beginning of its discovery, the carbon nanotube

has been regarded as an ideal material for electron field emitter. The advantage of the carbon nanotube as an electron emitter lies in the fact that the nanotube is very good conductor with a high aspect ratio and, consequently, consumes very small power in the field emission of electrons. Many experiments with single-walled (38,39) and multiwalled (40-44) carbon nanotubes have demonstrated such advantage.

In addition to much low extraction voltage, several characteristic features have been reported for carbon nanotube field emission. In this section, we describe them by noting the differences from the micron-sized metal tip emitters. Fowler-Nordheim theory (45), which is based on one-dimensional WKB approximation, predicts a linear behavior in the plot of $Ln(1/V^2)$ $Log(1/V^2)$. Experimental results on the micron-sized metal tip have shown excellent linear Fowler-Nordheim plots, which means that, since the dimension of the cross-section of micron-sized tip is much larger than the electron wave length, one-dimensional approximation ignoring the xy variation is relevant in that size range (46). However, many experiments on carbon nanotube field emission have demonstrated a nonlinear Fowler-Nordheim plot (47-49). Dean *et al*. argued that the nonlinear Fowler-Nordheim plot results from the displacement of adsorbates (50).

The energy distribution of the emitted electron in the micron-sized metal tip is asymmetric with respect to its peak position which is pinned at the Fermi level of the emitter (46), which is very consistent with the prediction of Fowler-Nordheim theory. However, in the cases of nanotube emitters, the distribution is sharper and rather symmetric with respect to its peak and the peak position shift down as the applied field increases (51). An additional characteristics of the carbon nanotube field emission is that the emission current is sensitively dependent on the adsorption states. Most of the emission images show lobes which is believed to reflect the presence of adsorbates (52). When the nanotube field emitter is heated to about 900K, a rapid drop in the magnitude of the emission current is observed. A subsequent cooling to room temperature recovers the initial amount of the current. This rapid drop in the magnitude of the current at high temperature is concurrent with the rapid change of the images from bright lobes to dimmer blurred images. These facts have been believed to be a firm evidence for the current enhancement by the adsorptions and the localized states (52).

However, experiments on gas adsorptions reported puzzling effects on carbon nanotube field emitter with oxygen adsorbates; the short time exposure to O_2 or H_2O induces an increase in the emission current, whereas the long time exposure can induce an irreversible current degradation (53). The oxygen adsorption on the micron-sized metal tip is known to reduce the emission current by inducing a surface dipole which increases the work function (54).

In **Fig 4**, we present our calculational results on the model geometries. Here we consider two types of adsorptions,

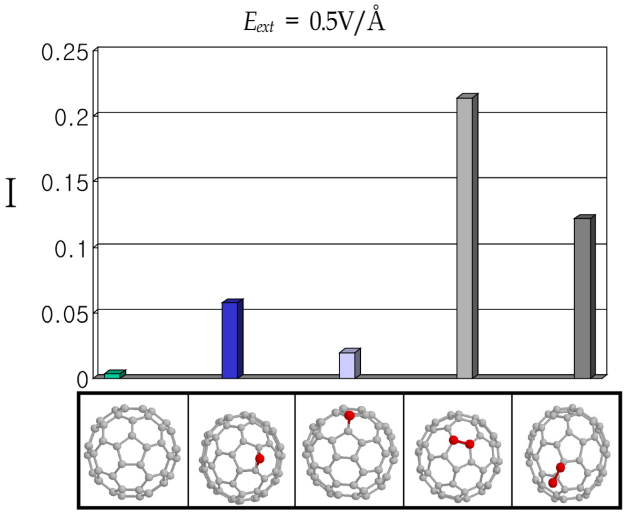

Fig 4. The calculated field emission current (in μA) for the (5,5) carbon nanotube with or without oxygen adsorbates. The length of the nanotube used in the calculation is about 30 Å and only top views of the tubes are shown. Grey small spheres represent carbon atoms and red spheres represent oxygen atoms.

atomic or molecular, as possible configuration of oxygen on the nanotube tip. The details for calculational method can be found in the reference (55). Based on these data, we conclude that the oxygen adsorption can generally increase the field emission from the carbon nanotube. Especially the increase of the emission current by two orders of the magnitude on the molecular adsorption is consistent with the abrupt changes in the magnitude of the emission current in the experiments.

Through detailed analysis on the electronic structure, we

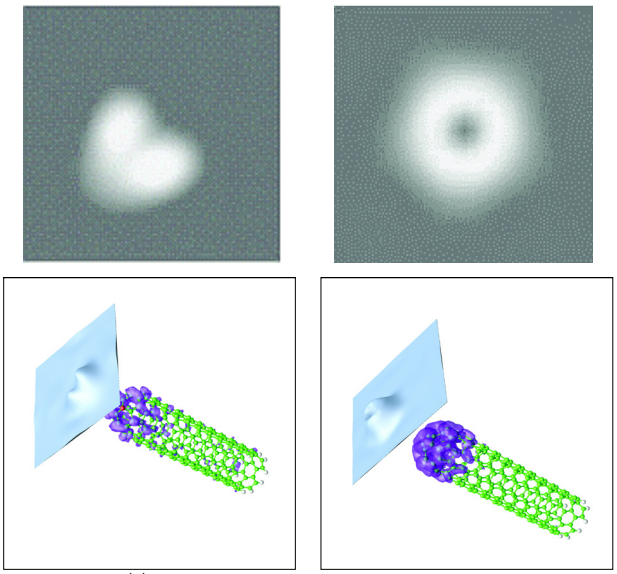

Fig 5. The calculated field emission images for (a) the case of atomic adsorption and (b) the case of bare carbon nanotube.

characterize two crucial factors for field emission at the nano-tip; one is local electric field and the other is local density of states nearby the Fermi level. The binding of the atomic adsorption is strong and the local density of states at the Fermi level is not so much different from that of the bare tube because the oxygen valence states (p) are located much below the Fermi level. In the case of molecular adsorptions, oxygen $pp\pi^*$ states give rise to much increase in the local density of states. However, the local electric fields are increased in both cases of atomic or molecular adsorption, which is ascribed to the electronegativity of oxygen adsorbates. Consequently, the atomic adsorptions induce an increase in the emission current by one order of magnitude and the molecular adsorption does by two orders of magnitude. The field emission images are calculated to confirm the nature of the image reported in the experiments. The images are obtained by visualizing the square of the electronic wave function at the anode plane which is assumed to be perpendicular to the tube axis. As shown in **Fig 5**, lobed images in various shapes represent dominantly emitting states rather than the geometrical shape of the tip and adsorbates.

Ⅴ. Conclusion

First-principles computational studies of the carbon nanostructures were reviewed. Detailed comparison between large fullerenes structures and the capped nanotube structures was realised by the large scale density functional calculationswith localized basis. Algorithm and the excellent performance of the localized-basis computational packages were described with the comparison with that of the plane-waves. Based on the first-principles computational results, the curvature energy of the sp^2-bonded graphitic surfaces was modelled. It was found that C_{240} and the cap of (10, 10) nanotube have the most energetically favourable curvatures, which could explain the diameter distributions of the single-walled carbon nanotubes. Field emission properties of the carbon nanotube are also investigated. We find that the governing factor for the field emission current could be decomposed into the local electronic density of states and the local field enhancement factor. We found that oxygen adsorbates on the tip of carbon nanotube increase the local density of states in come cases, while they enhance local electric field in most cases owing to the stronger electronegativity.

References

(1) Kroto HW, Heath JR, O′ Brien SC, Curl RF, Smalley RE (1985) Nature **328,** 162
(2) Iijima S (1991) Nature **354**, 56
(3) Krätschmer W, Lamb LD, Fostiropoulos K, Hoffman DR (1990) Nature **347**, 354
(4) Dresselhaus MS, Dresselhaus G, Eklund PC, "Science of Fullerenes and Carbon Nanotubes", Academic Press, 1996
(5) Smith BW, Monthioux M, Luzzi DE (1998) Nature **396**, 323
(6) Hirahara K, Suenaga K, Bandow S, Kato H, Okazaki T, Shinohara H, Iijima S (2000) Phys. Rev. Lett. **85**, 5384
(7) Saito S, Sshiyama A (1991) Phys. Rev. Lett. **66**, 2637
(8) Jost MB, Troullier N, Poirier DM, Martins JL, Weaver JH (1991) Phys. Rev. B **44**, 1966
(9) Hamada N, Sawada S, Oshiyama A (1992) Phys. Rev., Lett. **68**, 1579
(10) Hebard AF et al.(1991) Nature **350**, 632

(11) Schluter M, Lannoo M, Needels M, Baraff GA, Tománk D (1992) Phys. Rev. Lett. **68**, 526
(12) Lee NS, Chung DS, Kang JH, Kim HY, Park SH, Jin YW, Choi YS, Han IT, Park NS, Yun MJ, Jung JE, Lee CJ, You JH, Jo SH, Lee CG, Kim JM (2000) Jpn. J. Appl. Phys. **39**, 7154
(13) Bonard J, Kind H, Stöckli T, Nilsson L (2001) Sold State Electronics **45**, 893
(14) Tans SJ, Verschueren ARM, Dekker C (1998) Nature **393**, 49
(15) Wong SS, Joselevich E, Woolley AT, Cheung CL, Lieber CM (1998) Nature **394**, 52
(16) Frank S, Poncharal P, Wang ZL, de Heer WA (1998) Science **280**, 1744
(17) Wildöer JWG, Venema LC, Rinzler AG, Smalley RE, Dekker C (1998) Nature **391**, 59
(18) Odom TW, Huang J, Kim P, Lieber CM (1998) Nature **391**, 62
(19) Hohenberg P, Kohn W (1964) Phys. Rev. **136**, B864
(20) Kohn W, Sham LJ (1965) Phys. Rev. **140**, A1133
(21) Park N, Lee K, Han S, Yu J, Ihm J (2002) Phys. Rev. B **65**, 121405
(22) Ihm J, Zunger A, Cohen ML (1979) J. Phys. C **12**, 4409
(23) Kenny SD, Horsfield AP, Fujitani H (2000) Phys. Rev. B **62**, 4899
(24) Iijima S, Ichihashi T (1993) Nature **363**, 603
(25) Kiang C, Goddard III WA (1996) Phys. Rev. Lett. **76**, 2515
(26) Thess A, Lee R, Nikolaev P, Dai H, Pett P, Robert J, Xu C, Lee YH, Kim SG, Rinzler AG, Colbert DT, Scuseria GE, Tománk D, Fischer JE, Smalley RE (1997) Science **273**, 483
(27) Cowley JM, Nikolaev P, Thess A, Smalley RE (1997) Chem. Phys. Lett. **265**, 379
(28) Bandow S, Asaka S, Saito Y, Rao AM, Grigorian L, Richter E, Eklund PC (1998) Phys. Rev. Lett. **80**, 3779
(29) Zhang Y, Gu H, Iijima S, Appl (1998) Phys. Lett. **73**, 3827
(30) Kanzow H, Lenski C, Ding A (2001) Phys. Rev. B **63**, 125402
(31) Rotkin SV, Suris RA (1999) Phys. Lett. A **261**, 98
(32) Krishnan A, Dujardin E, Treacy MMJ, Hugdahl J, Lynum S, Ebbesen TW (1997) Nature **388**, 451
(33) Adams GB, Shankey OF, Page JB, O'Keeffe M, Drabold DA (1992) Science **256**, 1792
(34) Tománek D, Zhong W, Krastev E (1993) Phys. Rev. B **48**, 15461
(35) Maiti A, Brabec CJ, Bernholc J (1993) Phys. Rev. Lett. **70**, 3023
(36) York D, Lu JP, Yang W (1994) Phys. Rev. B **49**, 8526
(37) Lu JP, Yang W (1994) Phys. Rev. B **49**, 11421
(38) Saito Y, Hamaguchi K, Nishino T, Hata K, Tohji K, Kasuya A, Nishina Y (1997) Jpn. J. Appl. Phys. **36**, L1340
(39) Bonard J, Salvetat J, STockli T, de Heer WA (1998) Appl. Phys. Lett. **73**, 918
(40) Rinzler AG, Hafner JH, Nikolaev P, Lou L, Kim SG, Tománek D, Nordlander P, Colbert DT, Smalley RE (1995) Science **269**, 1550
(41) de Heer WA, Chatelain A, Ugarte D (1995) Science **270**, 1179
(42) Saito Y, Hamaguchi K, Uemura S, Uchida K, Tasaka Y, Ikazaki F, Yumura M, Kasuya A, Nishina Y (1998) Appl. Phys. A **67**, 95
(43) Wang QH, Corrigan TD, Dai JY, Chang RPH (1997) Appl. Phys. Lett. **70**, 3308
(44) Collins PG, Zettl A (1996) Appl. Phys. Lett. **69**; (1997) Phys. Rev. B **55**
(45) Fowler RH, Nordheim L (1928) Proc. Roy. Soc. Lond. A **119**, 173
(46) Binh V, Garcia N, Prucell ST (1996) Advances in Imaging and Electron Physics, **95**, 63
(47) Collins PG, Zettl A (1996) Appl. Phys. Lett. **69**, 1969; (1997) Phys. Rev. B, **55**, 9391
(48) Xu X, *et al*. (1999) Appl. Phys. Lett. **74**, 2549
(49) Dimitrijevic S, *et al*. (1999) Appl. Phys. Lett. **75**, 2680
(50) Dean KA, Chalamala BR (2000) Appl. Phys. Lett. **76**, 375
(51) Fransen MJ, van Rooy T, Kruit P (1999) Appl. Surf. Sci. **146**, 312
(52) Dean KA, Chalamala BR (1999) J. Appl. Phys. **85**, 3832
(53) Dean KA, Chalamala BR (1999) Appl. Phys. Lett. **75**, 3017
(54) Chalamala BR, Wallace RM, Gnade BE (1998) J. Vac. Sci. Technol. B **16**, 2859
(55) Park N, Han S, Ihm J (2001) Phys. Rev. B **64**, 125401
(56) Ueno H, Osawa S, Osawa E, Takeuchi K (1998) Fullerene Science and Technology, **6**, 319

(Received Jul 4, 2005; Accepted Sep 2, 2005)